



Trigger and analysis tools for Dark Matter search in CUORE-0

Gabriele Piperno for the CUORE Collaboration

Dipartimento di Fisica, Sapienza Università di Roma and Sezione INFN di Roma, Roma I-00185, Italy

Abstract

The CUORE and CUORE-0 experiments have the possibility to search for Dark Matter interactions. To reach this goal is necessary to use a dedicated trigger, the Optimum Trigger, based on the matched filter technique, that pushes the energy threshold down to the keV region, where the signal is expected to lie. In addition, new low energy analysis tools are described.

Keywords: Dark Matter, CUORE, Bolometer

1. Introduction

The actual Universe is estimated to be energetically composed at 23 % by Dark Matter (DM), while ordinary matter represents only the 4 % [1]. Despite this, DM nature is not yet known, thus its search is a very active research fields in contemporary physics. The most expected DM candidates are the Weakly Interacting Massive Particles (WIMPs) [2]. Since the DM observation would be a milestone in particle physics, many experiments are optimized to search for a signal of interaction with this particular kind of non-Standard Model matter.

To have chances to see a DM interaction using the direct detection approach (record a nuclear recoil of a target nuclei via elastic scattering with DM in the keV region), some requirements must be fulfilled by the detector:

- large target mass,
- good energy resolution,
- low background,
- low energy threshold.

CUORE (see other proceeding of this conference and [3]) is an experiment that will will have all these qualities. This experiment, originally intended for Neutrinoless Double Beta Decay (NDBD) of ^{130}Te search, will be made by 988 TeO_2 crystals (for a total mass of 741 kg) grouped in 19 towers and will start data taking in 2015 in the Hall A of the underground Laboratori Nazionali del Gran Sasso (LNGS), Italy.

A single tower prototype, named CUORE-0 [4], is taking data since march 2013. This detector, in addition to the large mass, matches also the other “physical” required properties, since it features a very good energy resolutions (baseline resolutions are typically below 4 keV FWHM) and a background reduction is achieved by means of stringent procedures to grow crystals, clean tower materials and assembly line

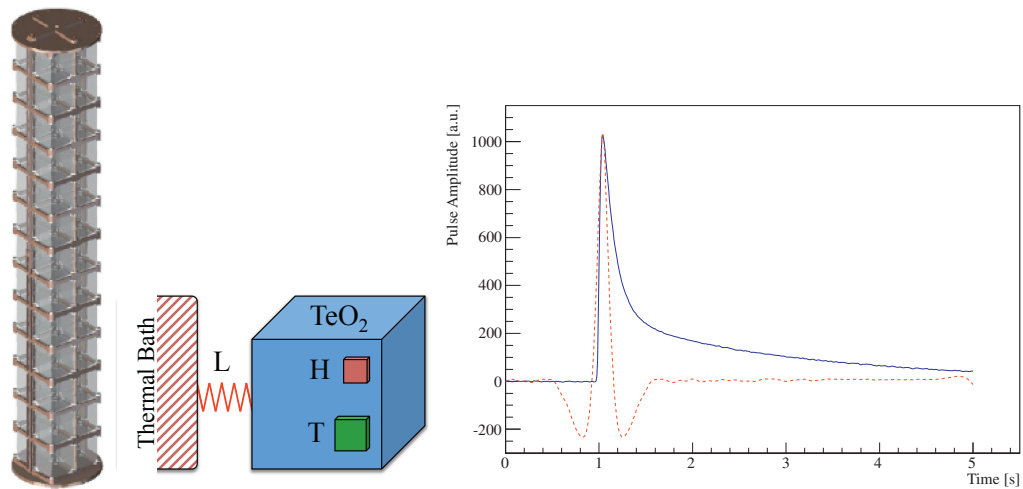


Fig. 1. Left: rendering of the CUORE-0 detector; the tower consists of $52 \times 5 \times 5 \text{ cm}^3$ TeO_2 crystals of 750 g each (for a total mass of 39 kg), arranged in 13 floors, in groups of 4 elements. Middle: single TeO_2 module schema with heater (H), thermistor (T) and link to the thermal bath (L) indicated. Right: a 2615 keV pulse, as come out from the detector (blue solid line) and filtered with the Optimum Filter (red dashed line).

instrumentation and by reducing any possible contamination risk. These three characteristics are mandatory as a result of the very low expected interaction rate, while a low energy threshold is needed since the signal should lie in the keV region of the energy spectrum (to look for an annual modulation of the interaction rate, like the DAMA experiment [5], and [6] for CUORE and CUORE-0).

In the following, after a presentation of the detector structure and operation, trigger and tools for the low energy analysis are described.

2. The CUORE-0 detector

CUORE-0 uses the bolometric technique to search for the NDBD of ^{130}Te : a bolometer is a calorimeter composed by two parts, an absorber and a sensor. In the crystal (the absorber) an energy release raises the temperature, while the sensor measures this temperature variation and then the energy deposited. The registered signal is pulse shaped and its height depends on the energy released (blue solid line in Fig.1 right). A good bolometer features a very low radioactive contaminations level and an excellent energy resolution: baseline resolution typically range from 1.5 to 4 keV FWHM.

The detector is hosted in the Hall A of the LNGS and is composed of $52 \times 5 \times 5 \text{ cm}^3$ TeO_2 crystals of 750 g each, for a total mass of 39 kg, arranged in 13 floors, at a working temperature of 13 – 15 mK (rendering of the tower in Fig.1 left). Every crystal is equipped with a Neutron Transmutation Doped (NTD) germanium thermistor, used as temperature sensor and with an heater, to correct pulse amplitude variation due to temperature oscillation. The crystals are held in position by means of polytetrafluoroethylene (PTFE) brackets that act also as a weak thermal coupling to the thermal bath, i.e. to the copper structure that supports the tower (single bolometer scheme in Fig.1 middle).

CUORE-0 is the first CUORE-like tower, build to validate the crystals production method, the cleaning procedure of the materials and the assembly line adopted to reduce the detector background, in particular the main fraction due to smeared α particles. Concerning the crystals production, a dedicated growth protocol [7] and sea level transportation allowed contaminations from ^{238}U (^{232}Th) decay chain for bulk and surface to be less than $6.7 \cdot 10^{-7} \text{ Bq/kg}$ ($8.4 \cdot 10^{-7} \text{ Bq/kg}$) and $8.9 \cdot 10^{-9} \text{ Bq/cm}^2$ ($2.0 \cdot 10^{-9} \text{ Bq/cm}^2$) at 90% C.L., respectively [8]. To further reduce the background rate a series of tumbling, electropolishing, chemical etching, and magnetron plasma etching for the surface treatment for the material facing the crystals was selected. The resulting upper limits is $1.3 \cdot 10^{-7} \text{ Bq/cm}^2$ at 90% C.L. in both ^{238}U and ^{232}Th [9].

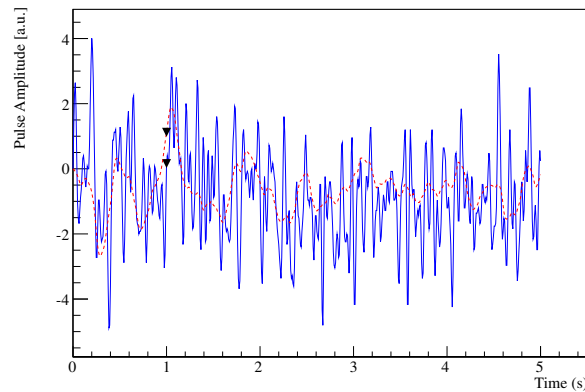


Fig. 2. A 3 keV pulse in a CUORE-0 channel. It is evident that the filtered pulse (red dashed line) is much less noisy with respect the original one (blue solid line). The black triangles indicate the trigger position, one for the original and one for the filtered pulse.

All the tower construction is performed in a class 1000 clean room inside glove boxes under nitrogen fluxing [10]. The mounted tower is enclosed in a copper thermal shield and located inside the Cuoricino (the CUORE demonstrator [11]) cryostat. In addition to the cryostat, also the external lead and borated-polyethylene neutron shielding and the Faraday cage are the ones used for Cuoricino. The front-end electronics and the data acquisition are identical too. All the signals produced by crystals are amplified and then filtered with a six-pole Bessel low-pass filter (cutoff at 12 Hz). Subsequently they are digitized using two 32-channel National Instruments PXI analog-to-digital converters with 125 S/s sampling rate, 18-bit resolution and 21 V range. The acquired data are both saved on disk and triggered in real time with a software generated trigger. The trigger generally employed in real time is the one intended for the high energy study (NDBD), while the one for the low energy analysis (DM) is ran over continuous data saved on disk.

3. Low energy trigger

3.1. Optimum Trigger

To detect DM interactions a low energy threshold trigger is needed. Given the very low event rate (tens of mHz) it is possible to use a trigger which is software generated. Using a trigger and a pulse shape algorithm based on the matched filter technique, which removes the non physical pulses, it has been demonstrated that is possible to push the energy threshold down to few keV [12]. The data buffer is divided into slices, filtered in the frequency domain and then triggered in the time domain. The trigger takes the name of Optimum Trigger (OT), while the filter is known as Optimum Filter (OF) and uses a transfer function that maximizes the signal to noise ratio:

$$H(\omega) = \frac{S^*(\omega)}{N(\omega)} e^{-i\omega t_m}$$

where $S^*(\omega)$ is the Discrete Fourier Transform of the average signal shape (taken from data), $N(\omega)$ the noise power spectrum (taken from data) and t_m is a parameter to adjust the delay of the filter. In Fig.1 right are presented the original pulse (solid blue line) and the one filtered using OF (dashed red line) for a 2615 keV event.

The OT works on filtered samples, which are less noisy with respect to the original ones, allowing to reach a very low threshold. As example in Fig.2 are shown, for a 3 keV pulse, the normal shape (blue solid line) and the filtered one (red dashed line).

A newer version of the OT than the one described in [12], with improved event selection and efficiency, has been developed. The optimization of the event selection is necessary since some non-physical pulses can deceive the trigger and make it fire. The major source of inefficiency of the old version of the OT is

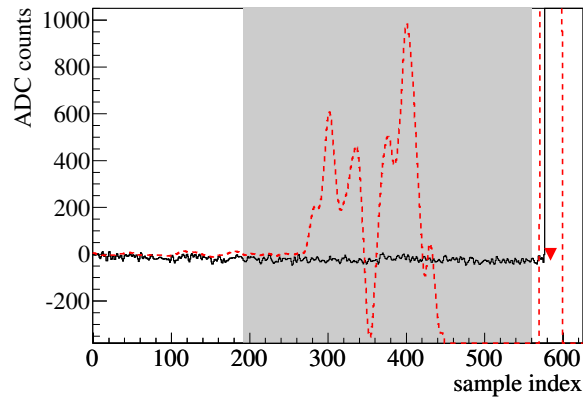


Fig. 3. A veto region (gray band) is present in the old version of OT to avoid the triggering of non physical pulses generated as secondary pulses when an high energy event occur. In black solid line the original pulse, in red dashed line the filtered one. The red triangle indicates the trigger position.

given by the presence of a veto in the trigger. The veto is required to avoid the triggering of non-physical secondary pulses: when an high energy event is triggered, a set of side pulses appear and these fake pulses can exceed the threshold and make the trigger fires again. This problem was solved putting a veto region on the sides lobes of the primary pulse, where is not possible to set a trigger (see Fig.3). Clearly when contaminations with high energy peaks are present (like ^{210}Po or ^{210}Pb) the veto becomes an important source of inefficiency, since the high energy peaks rate produces up to 10 % of dead time [6]. In this new version of OT the veto region has been removed and, to avoid the triggering of secondary pulses, a check event by event is performed, looking if it could have been generated as side by an higher pulse in the nearby.

To study the trigger efficiency as a function of the energy some dedicated measurements are necessary. These measures, called “n-pulses runs”, are done performing an energy scan by means of the heater glued on crystals. Then, the ratio $\frac{\text{triggered pulses}}{\text{fired pulses}}$, give the measure of the trigger efficiency. It is also possible to describe the trigger efficiency with a priori information since it is expected to follow the trend of a gaussian cumulative distribution function. Using the error function (erf), efficiency (Eff) for a single channel can be expressed as:

$$Eff(x) = \frac{1}{2} erf\left(\frac{x - OT_{thr}}{\sqrt{2}\sigma}\right) + \frac{1}{2}$$

with σ equal to the filtered baseline resolution and OT_{thr} equal to the OT threshold, generally set to $3 \times \sigma$ for CUORE-0. An example of the result of a heater scan measurement, with the expected efficiency trend superimposed, is shown in Fig.4. It is important to underline that the energy spectrum threshold is not mandatorily equal to the OT threshold, but it can be different and, for example, set equal to the value at which the 99% efficiency is reached, while it is evident from the previous equation that at OT_{thr} efficiency is always equal to 50%.

To further study the detector behavior, utilising the average pulse and the average noise, is possible to monitor run by run the filtered baseline resolution and the efficiency at the selected threshold (a physical run lasts about 24 h). The baseline resolution σ is obtained applying the OF to the noise of the run:

$$\sigma^2 = \sum_{k=0}^{M-1} h^2 \frac{|S(\omega_k)|^2}{N(\omega_k)}$$

where M is the acquired window length and h is a normalization constant to prevent the filter from modifying pulse amplitude. The efficiency can be inferred using the erf with the baseline resolution and the OF threshold corresponding to the selected run and then looking at the efficiency for the chosen spectrum energy threshold; the more the resolution is small (good) the more the efficiency is high, as can be seen in Fig.5.

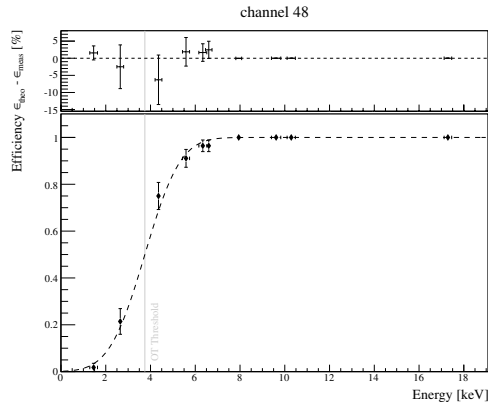


Fig. 4. OT trigger efficiency for channel 48 as a function of energy, measured in a dedicated n-pulses run in CUORE-0. In the lower part of the graph points represent the measured efficiency obtained by the ratio $\frac{\text{triggered pulses}}{\text{fired pulses}}$, the dashed black line is the expected efficiency trend and the vertical gray line is the OT threshold (50% efficiency for definition). In the upper part of the graph the residuals are shown.

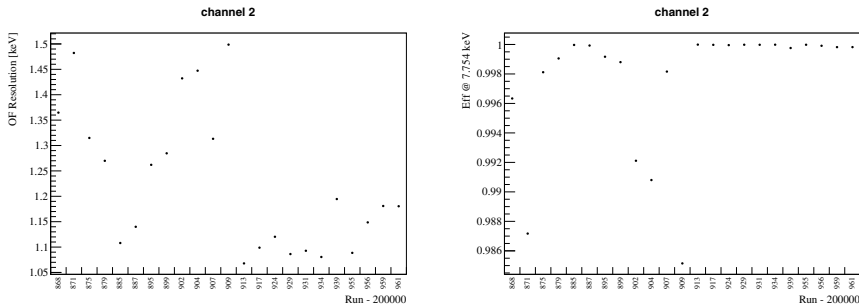


Fig. 5. Left: Using the average noise of each run is possible to monitor the OF baseline resolution run by run during data taking (channel 2 in the example). Right: taking this resolution is possible to estimate, by the *erf*, the trigger efficiency at a given energy (typically the threshold selected for that channel, in this case the channel 2).

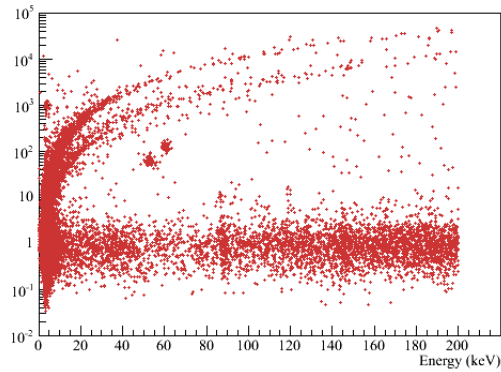


Fig. 6. SI obtained from the difference between the filtered pulse and the ideal filtered one (filtered average pulse) as function of the energy. The upper band is given by the spikes, while the lower one is given by the physical pulses.

3.2. Analysis tools

At low energy, spikes are a non negligible part of the background, and they cannot be discriminate by the trigger itself. Using a shape indicator (SI), like the one coming from the differences between each filtered pulse and the ideal filtered one (the average pulse), it is possible to remove such signals and more in general all the non-physical events; in formula:

$$SI = \sum_{i=0}^{L-1} \frac{(y_i^f - f_i)^2}{\sigma_L^2 (L-2)}$$

where y^f is the filtered signal, f is the ideal filtered one and σ_L is the amount of noise expected in a window of length L . In Fig.6 is shown the scatter plot of this shape indicator obtained for the low energy region.

However looking at this graph it is evident that at very low energy the SI described above is no longer able to discriminate good from bad pulses and so a new parameter becomes necessary. A possible solution is to use a bicomponent Optimum Filter: in addition to the noise power spectrum and the average (physical) pulse, this uses also the average spike to filter the data. Such a filter evaluates the fast (spike) and slow (physical) component of every pulse, which are given by:

$$\begin{pmatrix} \hat{A}_s(t_0) \\ \hat{A}_f(t_0) \end{pmatrix} = \begin{pmatrix} \sum |S_s|^2 N^{-1} & \sum (S_s^* S_f) N^{-1} \\ \sum (S_s^* S_f) N^{-1} & \sum |S_f|^2 N^{-1} \end{pmatrix}^{-1} \cdot \begin{pmatrix} \sum S_s^* e^{i\omega t_0} N^{-1} f \\ \sum S_f^* e^{i\omega t_0} N^{-1} f \end{pmatrix}$$

where $\hat{A}(t_0)$ is the best estimate of the amplitude in the time domain, S_s , S_f , N and f are to be intended in the frequency domain, with f and s subscripts indicating the fast and the slow component, respectively and the sums run over ω . For a more detailed explanation of the bicomponent OF look at [13]. As example in Fig.7 is shown a possible parameter, given by the amplitude ratio $\frac{\text{Fast-Slow}}{\text{Fast+Slow}}$, which optimization is ongoing.

4. Conclusions

Due to its large mass, good energy resolution and low background the CUORE experiment is very attractive for Dark Matter search. It will be composed by 19 towers for a total mass of 741 kg of TeO₂ crystals. A single tower prototype, CUORE-0, started to take data in march 2013 in the underground Laboratori Nazionali del Gran Sasso. Since the Dark Matter signal is expected to be well below 20 keV, a dedicated trigger is needed to push energy threshold down to this region. Using a trigger, called Optimum Trigger, based on

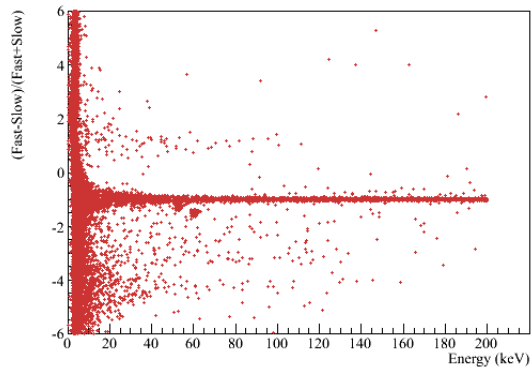


Fig. 7. Using the fast (spike) and the slow (physical) component of each pulse is possible to create new variables to discriminate events. As example is presented the ratio $\frac{\text{Fast}-\text{Slow}}{\text{Fast}+\text{Slow}}$, which discrimination power must be checked. The event distribution around the -1 horizontal line is given by the physical pulses.

the matched filter technique, is possible to reach such low energies, opening the possibility to search for an annual interaction modulation between Dark Matter and the detector.

In addition, the utilization of some analysis tools, as the SI, is necessary to discriminate physical from non-physical events in the low energy spectrum, reducing the background in the region of interest.

References

- [1] P. A. R. Ade *et al.*, *Planck 2013 results. I. Overview of products and scientific results*. arXiv:1303.5062, 279 (2005).
- [2] G. Steigman and M. S. Turner, *Cosmological constraints on the properties of weakly interacting massive particles*. Nucl. Phys. B, **253**, 375 (1985).
- [3] D. R. Artusa *et al.*, *Searching for neutrinoless double-beta decay of ^{130}Te with CUORE*. arXiv:1402.6072.
- [4] C. P. Aguiere *et al.*, *Initial performance of the CUORE-0 experiment*. arXiv:1402.0922.
- [5] R. Bernabei *et al.*, *DAMA/LIBRA results and perspectives*. arXiv:1403.1404.
- [6] F. Alessandria *et al.*, *The low energy spectrum of TeO_2 bolometers: results and dark matter perspectives for the CUORE-0 and CUORE experiments*. JCAP 01, **038** (2013).
- [7] C. Arnaboldi *et al.*, *Production of high purity TeO_2 single crystals for the study of neutrinoless double beta decay*. J. Cryst. Growth, **312**, 2999 (2010).
- [8] F. Alessandria *et al.*, *CUORE crystal validation runs: results on radioactive contamination and extrapolation to CUORE background*. Astropart. Phys., **35**, 839 (2012).
- [9] F. Alessandria *et al.*, *Validation of techniques to mitigate copper surface contamination in CUORE*. Astropart. Phys., **45**, 13 (2013).
- [10] M. Clemenza, C. Maiano, L. Pattavina, and E. Previtali, *Radon-induced surface contaminations in low background experiments*. Eur. Phys. J. C **71**, 1 (2011).
- [11] E. Andreotti *et al.*, *^{130}Te neutrinoless double-beta decay with CUORICINO*. Astropart. Phys., **34**, 822 (2011).
- [12] S. Di Domizio, F. Orio, M. Vignati, *Lowering the energy threshold of large-mass bolometric detectors*. JINST, **6**, P02007 (2011).
- [13] J. W. Beeman *et al.*, *Performances of a large ZnSe bolometer to search for rare events*. JINST, **8**, P05021 (2013).